Determination of the K_L for Laminar Flow in Square and Circular Pipe Fittings

By Ha Dinh and Lisa Dahl

Fall 2007
CHEM E 499, Finlayson

I. Introduction

The pressure drop coefficient K_L is a parameter used for calculating the excess pressure drop for laminar flow in non-standard geometries. K_L accounts for the bends in pipe geometries by scaling the normal pressure drop over a straight section of a square or circular pipe in fully developed flow. The fully-developed pressure drop is calculated using the Hagen Pouiseuille Law, where

$$\Delta p_{fd} = 32\frac{\eta L < v >}{d^2} \tag{A}$$

is used for a pipe with a circular cross-section, where _ is the viscosity, L is the length of the pipe, <*v*> is the average flow velocity in the pipe and *d* is the diameter of the pipe. For a square cross-section,

$$\Delta p_{fd} = 28.4\frac{\eta L < v >}{d^2} \tag{B}$$

is used, where the only difference is the coefficient of 28.4.

In order to find K_L values applicable to any size geometry, all parameters used in defining the model and calculating the pressure drop are under non-dimensional parameters. Under this condition, the non-dimensional pressure standard p_s is given by

$$\Delta p_s = \frac{\eta < v >}{d} \tag{C}$$

and the total excess pressure can be calculated using the following:

$$\Delta p_{excess} = p' p_s - \Delta p_{fd} \tag{D}$$

where p' is the inlet pressure measured in a standard non-dimensionalized model, which can be measured using a program such a COMSOL Multiphysics. Once the excess pressure drop is calculated, the excess pressure drop coefficient can be found by

$$K_L = \frac{\Delta p_{excess} d}{\eta < v >} \tag{E}$$

where the value of K_L is unitless. From this, the K_L values of several types of geometries can be tabulated and compared as examined in the following. The two conditions examined are for the K_L under a Reynolds number and flow viscosity equal to 1 and then the variation of K_L over Reynolds numbers ranging from 0 to 100.

The Reynolds number is related to the pressure drop in flow through the Navier-Stokes equation, which for the laminar flow cases discussed here is represented by:

$$Re\frac{\partial \mathbf{u}'}{\partial t'} + Re\mathbf{u}' \bullet \nabla' \mathbf{u}' = -\nabla' p' + \nabla'^2 \mathbf{u}' \qquad \text{(F)}$$

The kinematic viscosity is related to the Reynolds number by the following equation:

$$\eta = \frac{\rho u_s x_x}{Re} \qquad \text{(G)}$$

where Re is the Reynolds number, ρ is the density, u_s is the non-dimensional velocity standard and x_s is the non-dimensional distance standard. As the program COMSOL allows both the density and the viscosity to be specified, either can be solved for using equation G in order to vary the Reynolds number of the flow throughout the model. In the cases solved for, the Reynolds number was expressed as 10^x, where x ranged in value from 0 to 2. This gave a total Reynolds number range of 0 to 100, over which the change in K_L was plotted.

II. Model Used and Procedure

The model of Steady-State Navier-Stokes under the Chemical Engineering Module was used in COMSOL Multiphysics. Non-dimensional parameters were used to give a nonspecific solution. For all geometries examined, the density of the entire subdomain was set to 0 and the viscosity was set to 1 (slow flow or Stokes flow), or the density was set to 1 and the viscosity was set to 1/Re. In each model, the inlet surface boundary condition was set to laminar inflow/outflow to allow for fully developed flow throughout the pipe. All exterior walls were set to a no-slip boundary condition while the outlet at the top right was set to have normal flow with a pressure of 0.

All of the geometries examined are listed in Table 1, along with the lengths of their straight sections and entire centerline. Also listed are the fully developed pressure drops for each length case, calculated using Equations A and B.

Table 1: Geometries Modeled with Lengths and Fully Developed Pressure Drops

Pipe	Geometry	Straight Length	Centerline Length	Straight _p_{fd} (Pa)	Centerline _p_{fd} (Pa)
SQUARE	**45° ELL**	4.0	4.4	113.6	124.960
SQUARE	**180° TURN, SHORT**	12.0	14.0	340.8	397.600
SQUARE	**180° TURN, LONG**	20.0	22.0	568	624.800
CIRCULAR	**45° ELL, STANDARD RADIUS**	8.0	8.785	256.0	281.120
CIRCULAR	**45° ELL, LONG RADIUS**	8.0	9.178	256.0	293.696
CIRCULAR	**90° ELL, STANDARD RADIUS**	8.0	9.571	256.0	306.272
CIRCULAR	**90° ELL, LONG RADIUS**	8.0	10.356	256.0	331.392
CIRCULAR	**180° BEND, CLOSE RETURN**	8.0	9.571	256.0	306.272
CIRCULAR	**180° BEND, LONG RETURN**	12.0	13.571	384.0	434.272

All of the pipes had standard dimensionless diameters of 1. For the square pipe geometries, different straight section lengths were examined. The square 45° ell geometry had straight sections lengths of 2 on either side of the bend. The square short 180° turn had straight lengths of 4 on each side of the turn and in between them, whereas the square long 180° turn had straight lengths of 6. Figures 1 and 2 demonstrate the 3D models in COMSOL for the square pipe geometries, where the fully-developed streamlines are modeled using red lines.

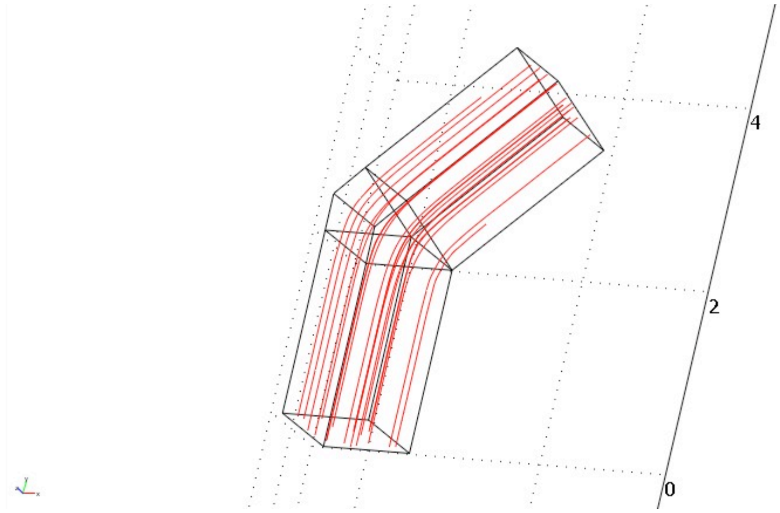

Figure 1: COMSOL Model of a Square Pipe with a 45° Ell

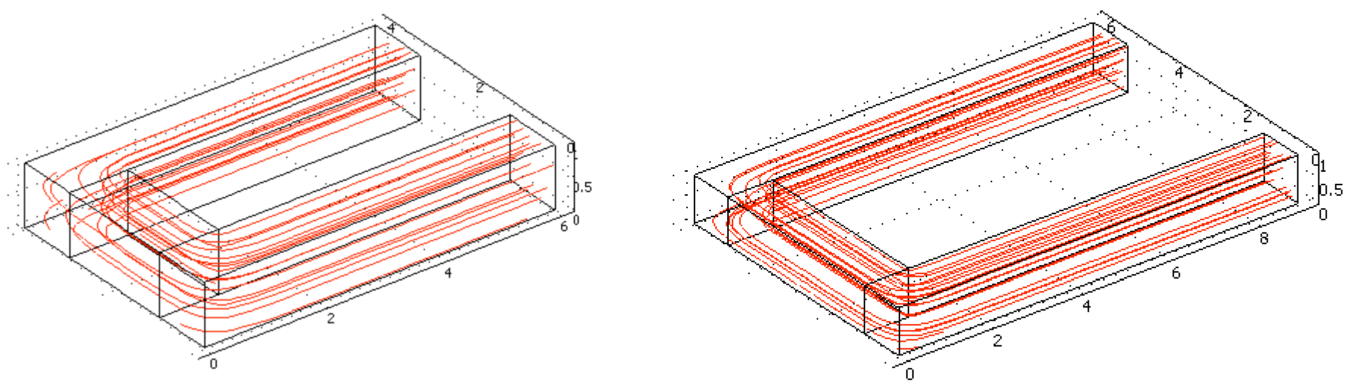

Figure 2: COMSOL Models of a Square Pipe with 180° Bend, short (left) and long (right)

All of the circular pipe geometries had straight section lengths of 4 whereas the radii of the bends were differentiated between short and long, based on standards listed in Perry's Chemical Engineering Handbook (Table 10-27). In general, a short radius has the same inner bend radius as the diameter of the pipe and a long radius has an inner bend radius equivalent to 1.5 times the diameter of the pipe. Figures 3 through 5 show all of the circular pipe geometries used including both the short and long radius versions.

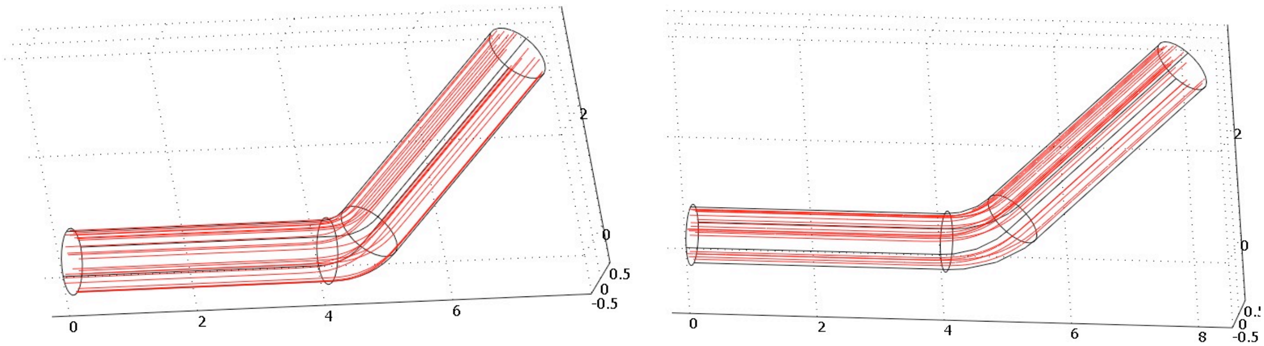

Figure 3: COMSOL Models of Circular Pipe with 45° Bend, short radius (left) and long radius (right)

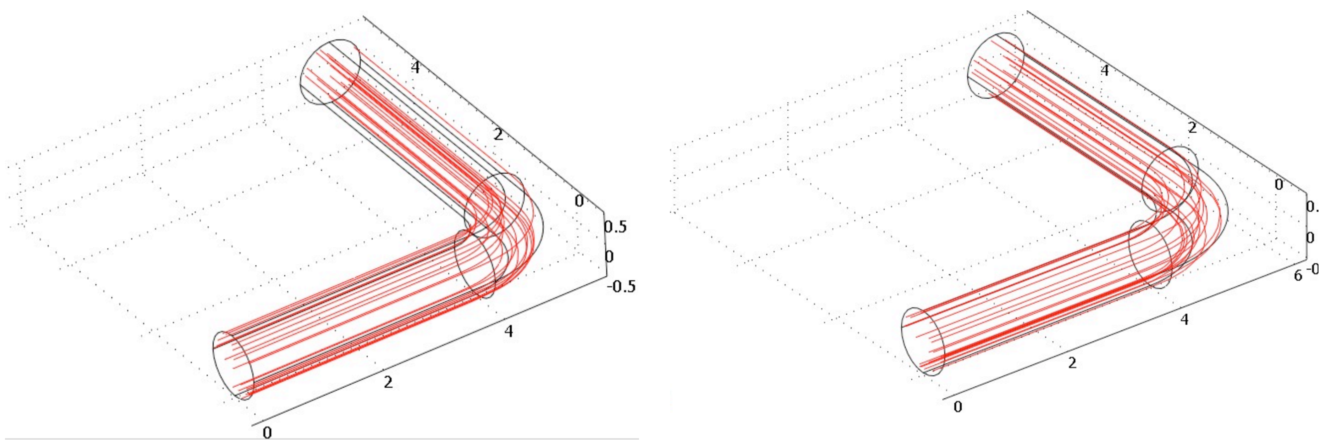

Figure 4: COMSOL Models of Circular Pipe with 90° Bend, short radius (left) and long radius (right)

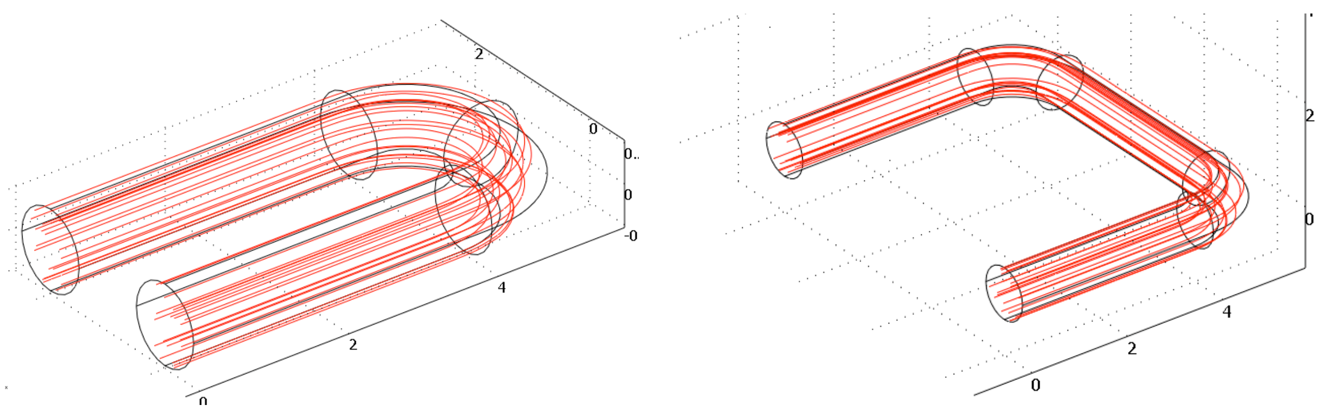

Figure 5: COMSOL Models of Circular Pipe with 180° Bend, close return (left) and long return (right)

Streamlines were plotted for all of the geometries at a Reynolds number of 100 to ensure fully developed flow was present throughout the entire pipe length in each case. The solved model then had its inlet pressure recorded and graphed over varying Reynolds numbers to solve for K_L.

III. Results and Discussion

All models were solved under three meshes of increasing complexity and degrees of freedom. As the final result K_L seemed to converge with a higher mesh, the results of the third mesh were used as the results. Table 2 lists the result of K_L for each geometry modeled.

Table 2: Final Results for the Excess Pressure Drop Coefficient K_L

Pipe	Geometry	K_L (Straight Length)	K_L (Centerline Length)
SQUARE	**45° ELL**	10.4	-0.95
SQUARE	**180° TURN, SHORT**	41.2	-15.6
SQUARE	**180° TURN, LONG**	39.2	-17.6
CIRCULAR	**45° ELL, STANDARD RADIUS**	24.9	-0.2
CIRCULAR	**45° ELL, LONG RADIUS**	37.5	-0.2
CIRCULAR	**90° ELL, STANDARD RADIUS**	49.8	-0.4
CIRCULAR	**90° ELL, LONG RADIUS**	75.1	-0.3
CIRCULAR	**180° BEND, CLOSE RETURN**	100	49.8
CIRCULAR	**180° BEND, LONG RETURN**	86.4	29.6

Two K_L values were considered for these results. The first K_L value is known as the "straight length" value where the pressure drop including only the length of the straight sections of the pipe were subtracted from the excess pressure found through COMSOL. The second value subtracts a pressure drop which includes the entire centerline length of the pipe, assuming fully developed plow along the axis. Most of the cases, particularly the 45° and 90° geometries, have lower K_L values when the centerline length is included. This is expected because fully developed flow should be present throughout most of the pipe, and any excess changes in pressure should be due to changes in the flow directly near the deviations in the geometries.

More unpredictable values for the K_L values are exhibited in the geometries with 180° turns or bends. In all four cases listed in Table 2, very large K_L values are seen even when the entire centerline of the pipe is included. This could possibly be due to the sharp changes in direction and momentum for the fluid in the pipe, which should have some contribution to the overall pressure drop of the fluid.

Also of note is that negative K_L values have little meaning with regards to calculating the excess pressure drop in an abnormal geometry. Therefore, all negative values found in the results over varying Reynolds numbers were graphed with their absolute values only. Figures 6 to 14 show how the value of K_L changes under each geometry and length consideration (straight or centerline), where any negative K_L values are graphed using a dashed line. All plots are under a log-log axes to examine for any linear variation.

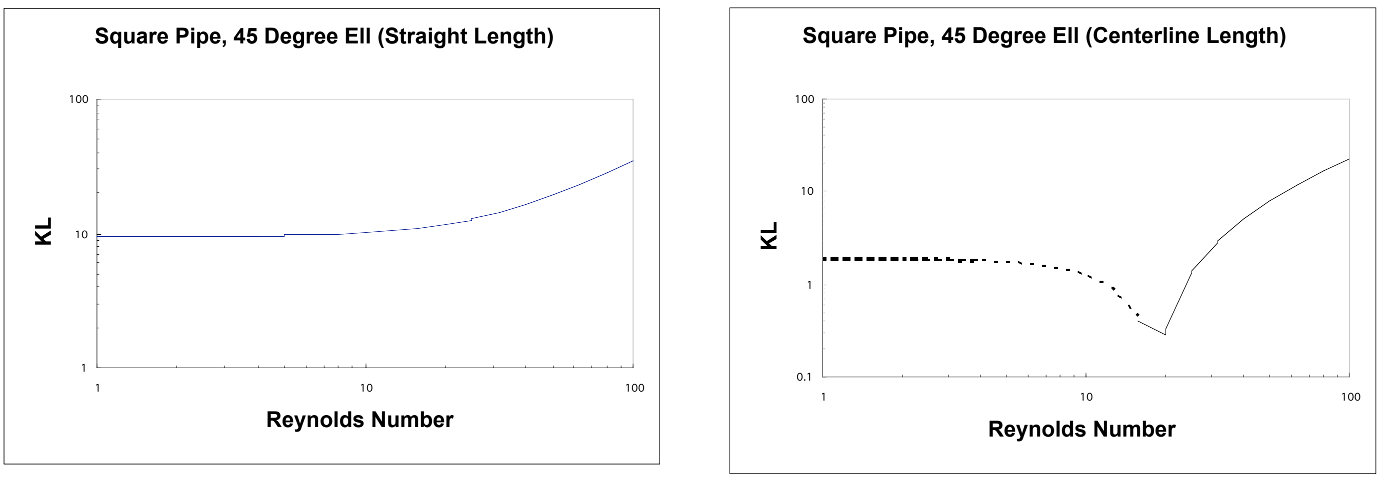

Figure 6: K_L over varying Re for the square 45° bend model, straight (left) and centerline (right)

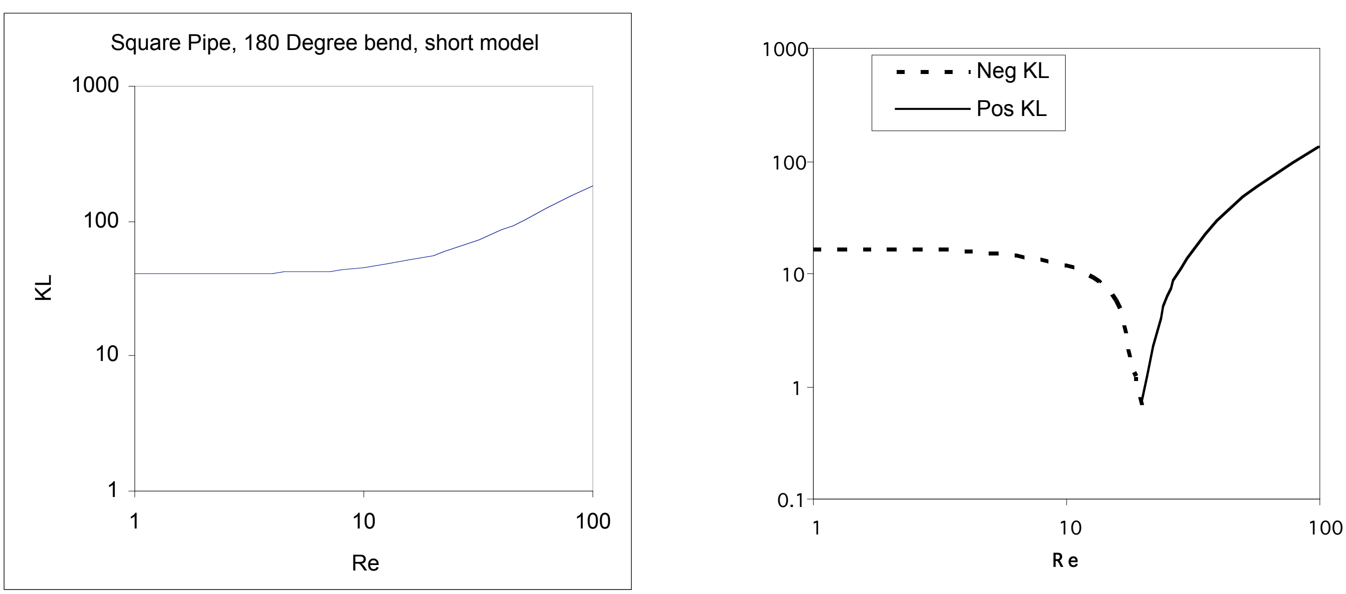

Figure 7: K_L over varying Re for the square 180° bend, short model, straight (left) and centerline (right)

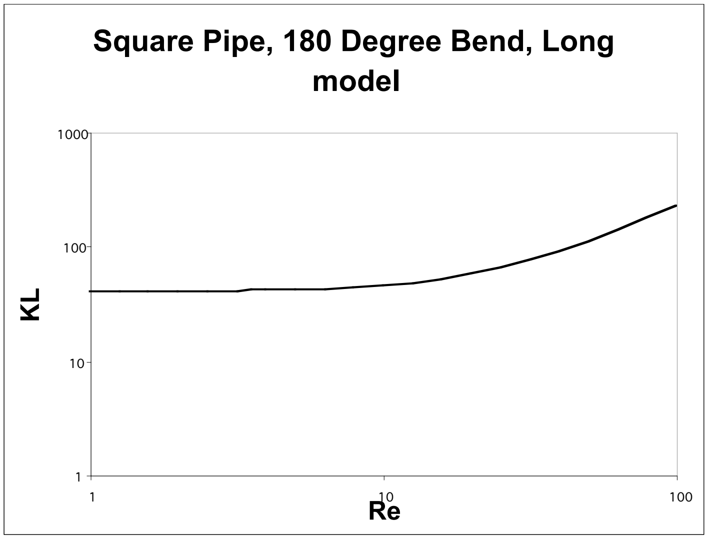

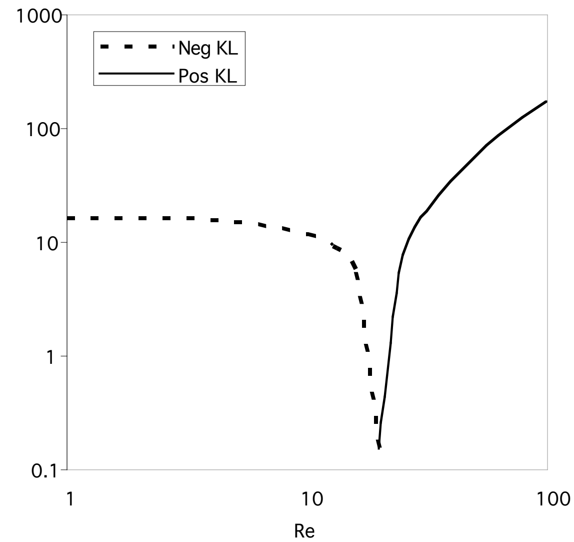

Figure 8: K_L over varying Re for the square 180° bend, long model, straight (left) and centerline (right)

All of the square pipe geometries demonstrate the same type of change over Reynolds number when the centerline is included in the fully developed pressure drop calculation. All K_L values for Reynolds numbers below the value 20 tend to be negative for all square geometries, while all solutions with Re greater than 20 have positive K_L values that increase very dramatically up to an Re equivalent to 100.

The circular pipe geometries show the same kind of negative-to-positive switch in K_L value at Reynolds numbers between 19 to 20 for the 45° bend models and 15 to 16 for the 90° bend models.

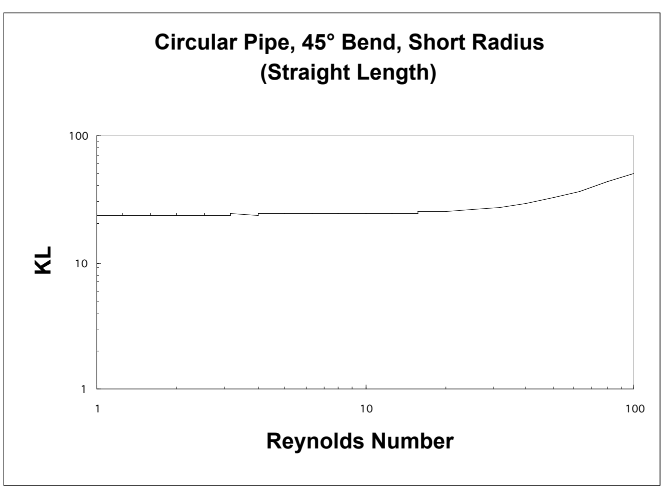

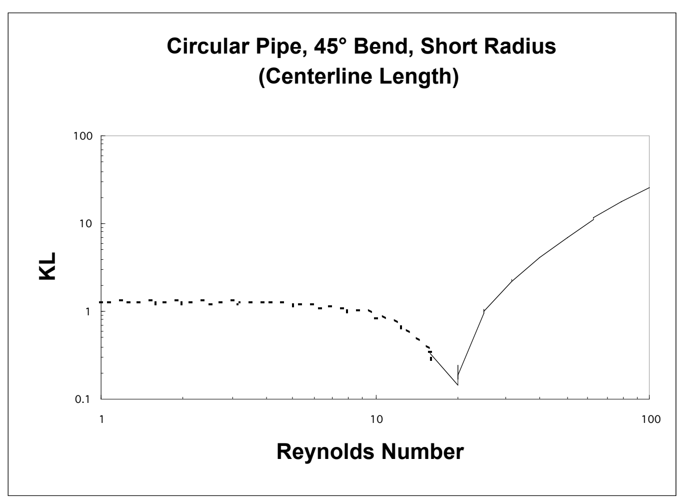

Figure 9: K_L over varying Re for the circular 45° short radius model, straight (left) and centerline (right)

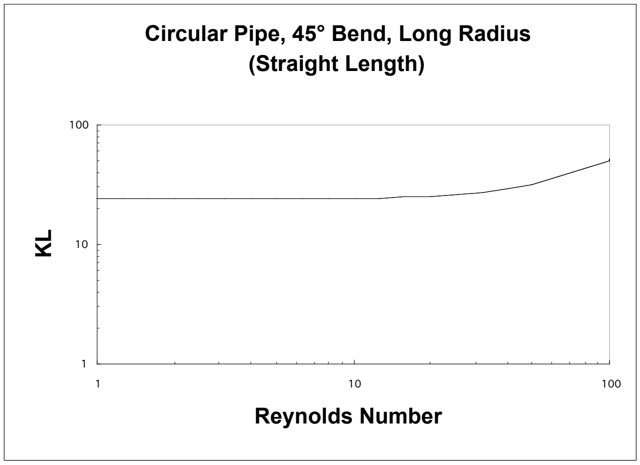

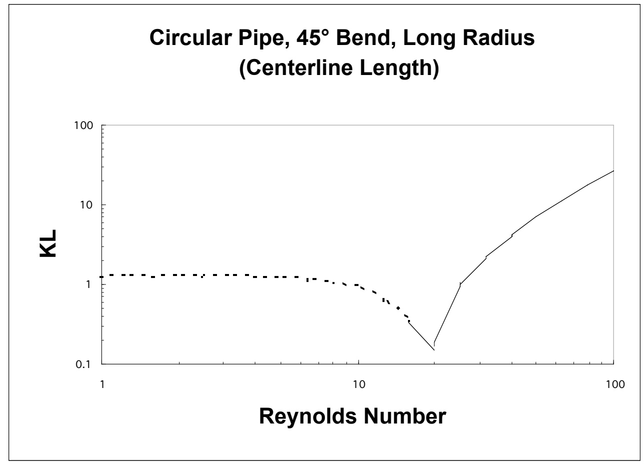

Figure 10: K_L over varying Re for the circular 45° long radius model, straight (left) and centerline (right)

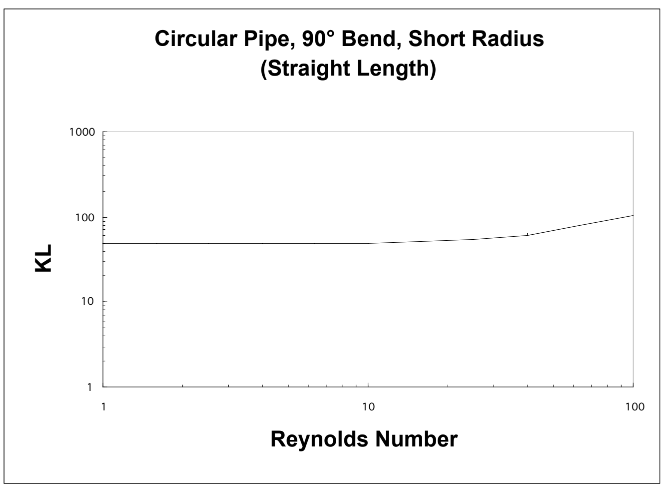

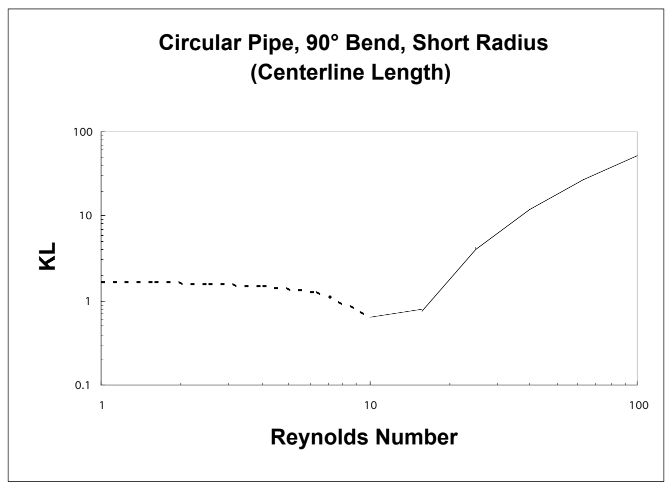

Figure 11: K_L over varying Re for the circular 90° short radius model, straight (left) and centerline (right)

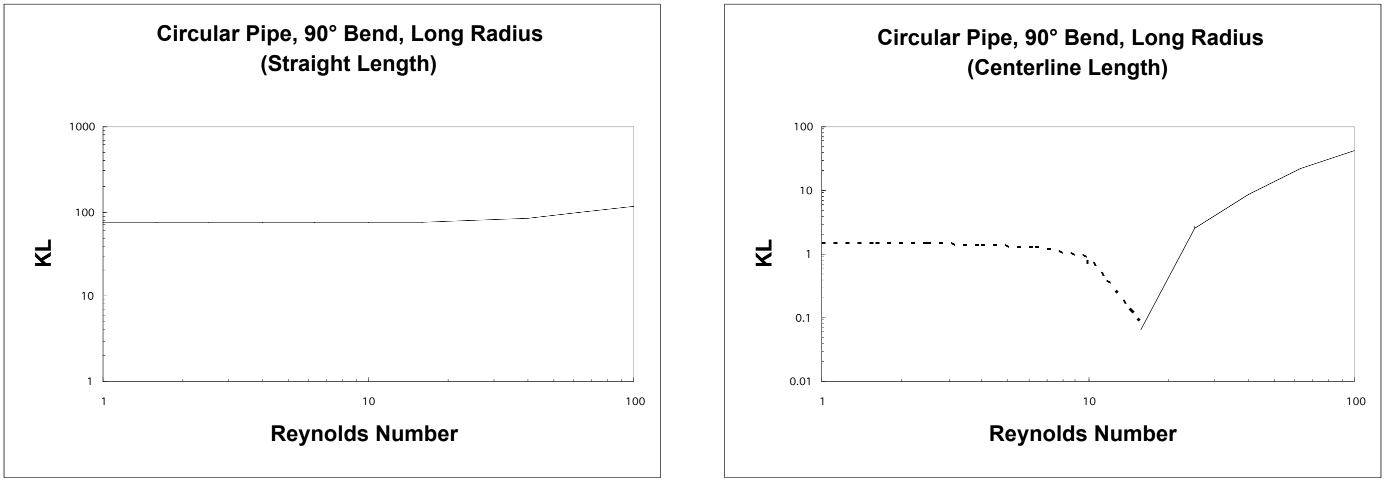

Figure 12: K_L over varying Re for the circular 90° long radius model, straight (left) and centerline (right)

In comparison to the trends shown by Figures 9 through 12, the 180° bend geometries exhibited similar behavior as demonstrated in Figure 13.

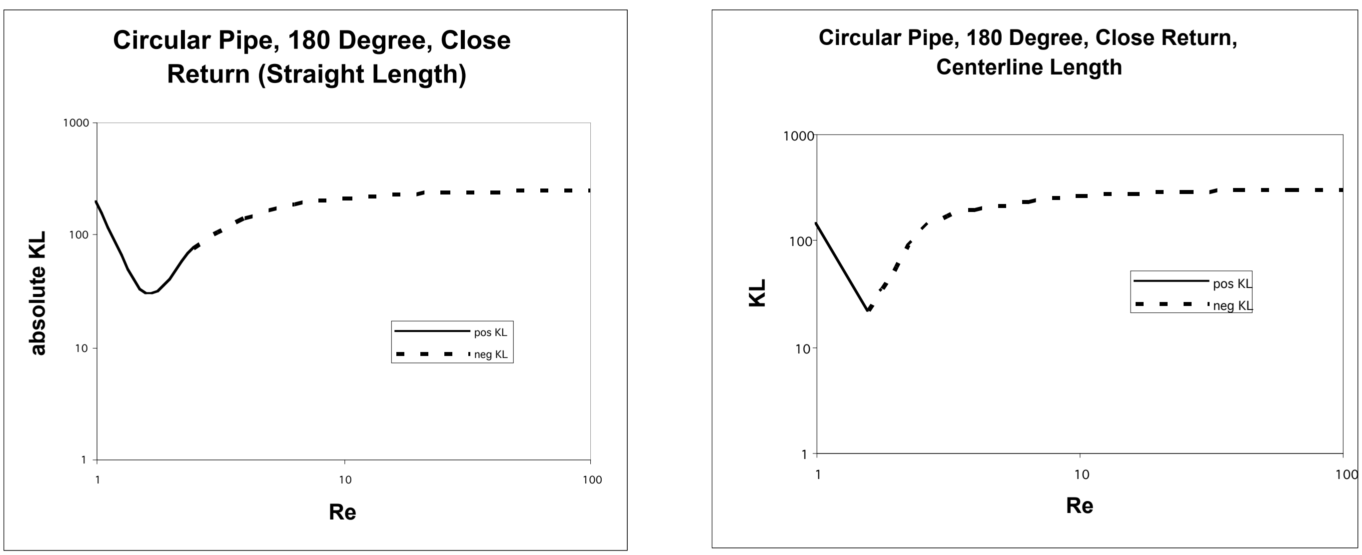

Figure 13: K_L over varying Re for the circular 180° short radius model, straight (left) and centerline (right)

In all cases, the K_L values over varying Reynolds numbers demonstrated similar trends, where increasing the Reynolds number generally led to increasingly negative K_L values past Re = 15 to 16. For the circular pipe 180° models this increase happened much more quickly, at about Reynolds numbers slightly over 2 as shown in Figure 13. In general, however, including the center-line length when calculating the fully-developed pressure drop over-accounts for the total pressure drop in the geometry, as demonstrated by the negative K_L values achieved in all cases for all high Reynolds numbers.

In most cases, the overall pressure coefficient results depicted in Table 2 show that including the length of the centerline when calculating the pressure drop of a fitting overaccounts for the total pressure difference, as shown through the negative values of the centerline pressure drop coefficients. The 180° turns show an opposite trend in that they have larger positive K_L values that become more negative as the Reynolds number is increased. Therefore, when calculating a dimensional, isolated pressure drop of a fitting with a 45° or 90° bend, it is recommended that the K_L found through using the straight lengths be used as opposed to the center-line values. This is because it the straight length coefficients account for the difference between the straight sections of the pipe and the fitting, so using this K_L with the corresponding Hagen-Pouiseuille equation will find the contribution to the pressure drop from the fitting only.

All of the Reynolds number analyses were performed at only a second mesh, so it is recommended that future research examines the variations at a third or fourth mesh in order to confirm the trends found above. In addition, recalculating the single K_L values at higher meshes for all of the pipe geometries will allow for a converging value to be determined. The overall results reported here are reported to one decimal point and can give a general idea of a fitting's contribution to the overall pressure drop in a pipe at any dimension, yet further analysis is beneficial to increasing the accuracy of these results.

References

1. Finlayson, Bruce A. *Introduction to Chemical Engineering Computing*. Hoboken: John Wiley & Sons, Inc., 2006.

2. Koch, M.V., VandenBussche, K. M., and Chrisman, R. W. *Micro Instrumentation*. Hoboken: John Wiley & Sons, Inc., 2007.

3. Bird, R.B., Stewart, W.E. and Lightfoot, E.N. *Transport Phenomena*. Second Edition. Hoboken: John Wiley & Sons, Inc., 2007.

Appendix

I. Sample Calculations

A. *Calculating the non-dimensional parameter p_s*

The non-dimensional parameter p_s is given by:

$$\Delta p_s = \frac{\eta < v >}{d}$$

$$\Delta p_s = \frac{(1)(1)}{(1)} = 1$$

B. *Calculating the fully developed pressure drop:*

The pressure drop was approximated using the Hagen-Pousiuelle law.
For fully developed flow, the pressure drop across a square straight pipe is given by:

$$\Delta p_{fd} = 28.4 \frac{\eta L < v >}{d^2}$$

The pressure drop across a circular, straight pipe with fully-developed flow is:

$$\Delta p_{fd} = 32 \frac{\eta L < v >}{d^2}$$

Example using the square pipe with a 45° ell:
Using only the straight, rectangular sections of the geometry: L = 2.0 + 2.0 = 4.0

$$\Delta p_{fd} = 28.4 \frac{\eta L < v >}{d^2} = 28.4 \frac{(1 Pa \cdot s)(4m)(1m/s)}{(1m)^2} = 113.6 Pa$$

Using only the length along the entire centerline of the pipe: L = 2.2 + 2.2 = 4.4

$$\Delta p_{fd} = 28.4 \frac{\eta L < v >}{d^2} = 28.4 \frac{(1 Pa \cdot s)(4.4m)(1m/s)}{(1m)^2} = 124.96 Pa$$

C. *Calculating the excess pressure due to the abnormal geometry:*

The excess pressure can be given by:

$$\Delta p_{excess} = p' p_s - \Delta p_{fd}$$

Where the pressure p' is measured by Comsol using boundary integration for pressure at the inlet, multiplied by the non-dimensional parameter p_s. For L = 4.0 (straight, rectangular sections only) with the second mesh:

$$\Delta p_{excess} = 124.005662 - 113.6 = 10.4\,\mathrm{s}$$

For L = 4.4 (including the entire pipe centerline) with the second mesh:

$$\Delta p_{excess} = 124.005662 - 124.96 = -0.95$$

D. *Calculating K_L using the excess pressure*:

The value of K_L is given by the equation:

$$K_L = \frac{\Delta p_{excess} d}{\eta < v >}$$

As all parameters except _p_{excess} are equal to 1, K_L = _p_{excess} with the values in C above.

E. *Relating the Reynolds number to the Kinematic Viscosity*

The Reynolds number is dependent on the kinematic viscosity by:

$$\mathrm{Re} = \frac{\rho u_s x_s}{\eta} = \frac{(1)(1)(1)}{\eta} = \frac{1}{\eta}$$

Therefore, the kinematic viscosity in the boundary conditions can be defined as:

$$\eta = \frac{1}{\mathrm{Re}} = \frac{1}{10^x}$$

Where x varies from 0 to 2 in increments of 0.1. This led to the solutions Figures 2 and 3 represent above.

II. Mesh Tables and Results for Each Geometry with _ = 1

SQUARE 45° ELL

	Mesh #1	Mesh #2	Mesh #3
Points	374	1090	3113
Elements	1305	4641	14436
DOF	12391	27885	72982
$p_{inlet} = p'p_s$	124.5842	124.1048	124.0056
$p_{excess} = K_L$	11.0 (-0.37)	10.5 (-0.86)	10.4 (-0.95)

SQUARE 180° TURN, SHORT

	Mesh #1	Mesh #2	Mesh #3
Points	--	--	--
Elements	874	2775	8110
DOF	5647	14431	40952
$p_{inlet} = p'p_s$	405.4624	383.9993	381.9864
$p_{excess} = K_L$	64.7 (7.9)	43.2 (-13.6)	41.2 (-15.6)

SQUARE 180° TURN, LONG

	Mesh #1	Mesh #2	Mesh #3
Points	--	--	--
Elements	2896	7639	20578
DOF	15809	39686	101097
$p_{inlet} = p'p_s$	617.1850	611.6224	609.2034
$p_{excess} = K_L$	49.2 (-7.6)	43.6 (-13.2)	39.2 (-17.6)

CIRCULAR 45° ELL, STANDARD RADIUS

	Mesh #1	Mesh #2	Mesh #3
Points	758	2166	6434
Elements	2591	9594	29848
DOF	14775	46261	140151
$p_{inlet} = p'p_s$	280.6611	280.832	280.8731
$p_{excess} = K_L$	24.7 (-0.4)	24.8 (-0.3)	24.9 (-0.2)

CIRCULAR 45° ELL, LONG RADIUS

	Mesh #1	Mesh #2	Mesh #3
Points	804	2334	6795
Elements	2751	10323	31629
DOF	15679	49810	148288
$p_{inlet} = p'p_s$	293.1489	293.4766	293.5210
$p_{excess} = K_L$	37.1 (-0.5)	37.5 (-0.2)	37.5 (-0.2)

CIRCULAR 90° ELL, STANDARD RADIUS

	Mesh #1	Mesh #2	Mesh #3
Points	816	2381	6951
Elements	2794	10562	32320
DOF	15928	50871	151645
$p_{inlet} = p'p_s$	305.6111	305.7367	305.8322
$p_{excess} = K_L$	49.6 (-0.7)	49.7 (-0.5)	49.8 (-0.4)

CIRCULAR 90° ELL, LONG RADIUS

	Mesh #1	Mesh #2	Mesh #3
Points	878	2540	7459
Elements	3006	11200	34744
DOF	17136	54087	162938
$p_{inlet} = p'p_s$	330.8694	330.9703	331.0752
$p_{excess} = K_L$	74.9 (-0.5)	75.0 (-0.4)	75.1 (-0.3)

CIRCULAR 180° BEND, CLOSE RETURN

	Mesh #1	Mesh #2	Mesh #3
Points	961	2828	8305
Elements	3293	12589	38712
DOF	18758	60531	181340
$p_{inlet} = p'p_s$	279.3635	279.4116	279.4761
$p_{excess} = K_L$	99.9 (49.6)	99.9 (49.7)	100 (49.8)

CIRCULAR 180° BEND, LONG RETURN

	Mesh #1	Mesh #2	Mesh #3
Points	1264	3642	10866
Elements	4331	16336	50593
DOF	1009	78247	237079
$p_{inlet} = p'p_s$	379.7859	379.85425	379.9244
$p_{excess} = K_L$	99.8 (49.5)	86.3 (29.5)	86.4 (29.6)